Supporting Information for QMrebind: Incorporating quantum mechanical force field reparameterization at the ligand binding site for improved drug-target kinetics through milestoning simulations

Anupam A. Ojha, Lane W. Votapka, and Rommie E. Amaro*

Department of Chemistry, University of California San Diego, La Jolla, CA, USA

E-mail: ramaro@ucsd.edu

Table S1: Unbinding rate constants (s^{-1}) for host-guest complexes obtained through QMrebind-reparameterized force field and the generic force field parameters employed in SEEKR2 simulations.

Host-guest complex	Experimental k_{off} (s^{-1})	QMrebind+SEEKR2 k_{off} (s^{-1})	SEEKR2 k_{off} (s^{-1})
BCD-1-propanol	$(1.21 \pm 0.07) \times 10^8$	$(1.94 \pm 0.01) \times 10^8$	$(5.31 \pm 0.02) \times 10^8$
BCD-1-butanol	$(3.8 \pm 0.6) \times 10^7$	$(5.53 \pm 0.02) \times 10^7$	$(7.24 \pm 0.02) \times 10^7$
BCD-methyl butyrate	$(1.28 \pm 0.03) \times 10^7$	$(1.87 \pm 0.01) \times 10^7$	$(3.48 \pm 0.01) \times 10^7$
BCD-tertbutanol	$(8.5 \pm 0.1) \times 10^6$	$(9.40 \pm 0.04) \times 10^6$	$(1.46 \pm 0.01) \times 10^7$
BCD-aspirin	$(1.31 \pm 0.03) \times 10^6$	$(3.04 \pm 0.02) \times 10^6$	$(5.82 \pm 0.03) \times 10^6$
BCD-1-naphthylethanol	$(5. \pm 2.) \times 10^5$	$(7.42 \pm 0.06) \times 10^5$	$(2.28 \pm 0.02) \times 10^6$
BCD-2-naphthylethanol	$(1.8 \pm 0.7) \times 10^5$	$(2.40 \pm 0.02) \times 10^5$	$(2.85 \pm 0.02) \times 10^5$

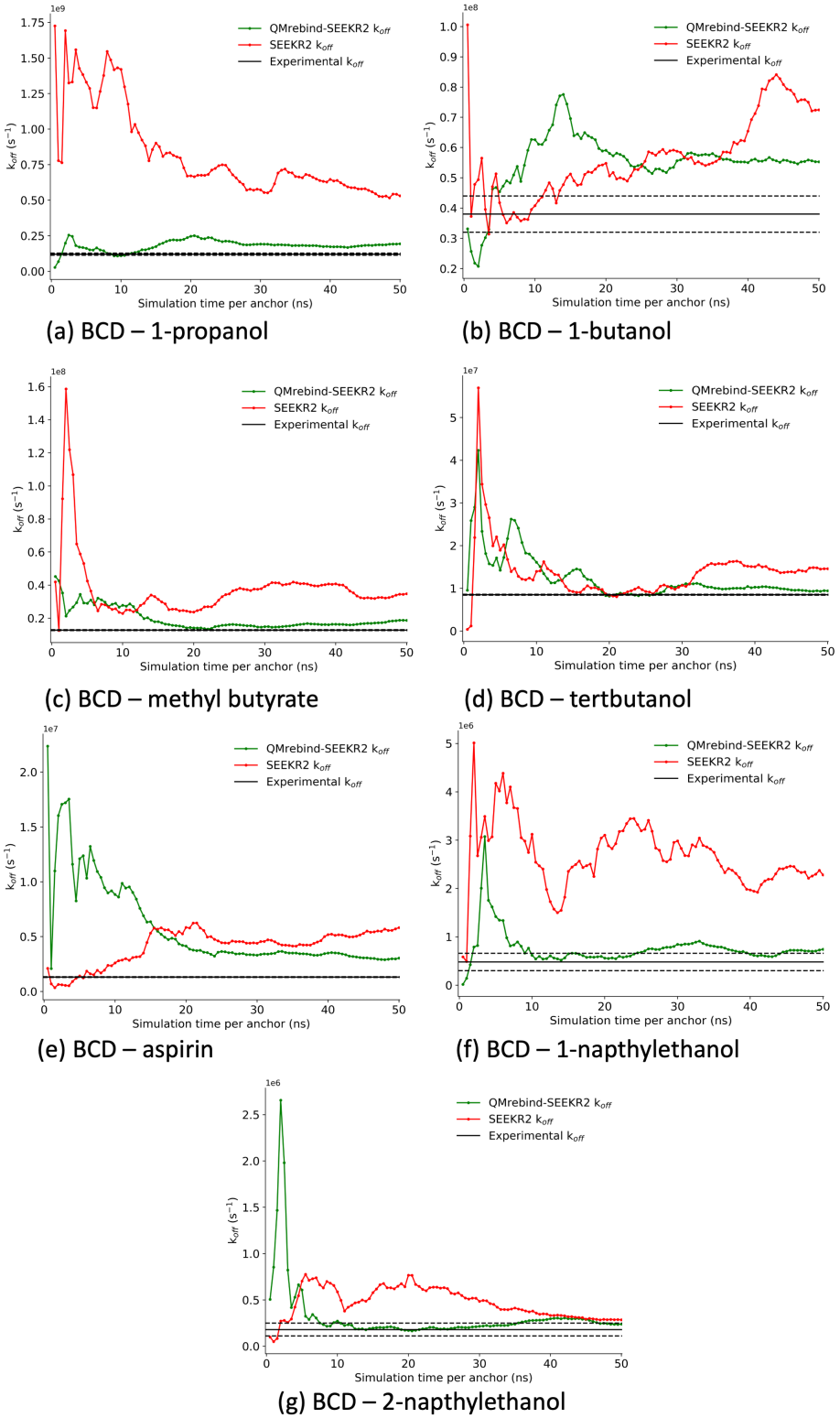

Figure S1: Evolution of receptor-ligand unbinding rate (k_{off}) for the seven host-guest complexes over simulation time for the QMrebind-reparameterized force field (in green) and the generic force field (in red) parameters employed in the SEEKR2 method. The experimentally obtained k_{off} values for the host-guest complexes are in black.

Table S2: Residues within 5 Å cut-off distance from the ligand for Hsp90-inhibitor complexes

Hsp90-inhibitor complex	Residues within 5 Å cut-off distance from the ligand
Hsp90-Ligand 1	Ile34, Asn36, Ser37, Ser38, Ala40, Leu41, Ile44, Val77, Thr79, Ile81, Gly82, Met83, Thr84, Lys85, Leu88, Ile89, Leu92, Gly93, Thr94, Ile95, Ala96, Gln118, Val121, Gly122, Phe123, Tyr124, Ile136, Lys138, Asn140, Thr169, Lys170, Ile172
Hsp90-Ligand 2	Ile34, Ser37, Ser38, Ala40, Leu41, Ile44, Val77, Thr79, Ile81, Gly82, Met83, Thr84, Lys85, Leu88, Gly93, Thr94, Ile95, Val121, Gly122, Phe123, Tyr124, Lys138, Asn140, Lys170, Ile172
Hsp90-Ligand 3	Ile34, Ser37, Ser38, Ala40, Leu41, Ile44, Val77, Thr79, Ile81, Gly82, Met83, Thr84, Lys85, Leu88, Gly93, Thr94, Ile95, Val121, Gly122, Phe123, Tyr124, Ile136, Lys138, Asn140, Lys170, Ile172
Hsp90-Ligand 4	Ile33, Asn35, Ser36, Ser37, Ala39, Leu40, Ile43, Val76, Thr78, Ile80, Gly81, Met82, Thr83, Lys84, Leu87, Gly92, Thr93, Ile94, Ala95, Gln117, Val120, Gly121, Phe122, Tyr123, Lys137, Asn139, Lys169, Ile171
Hsp90-Ligand 8	Ile33, Asn35, Ser36, Ser37, Ala39, Leu40, Ile43, Val76, Thr78, Ile80, Gly81, Met82, Thr83, Leu87, Gly92, Thr93, Ile94, Tyr123, Lys169, Ile171
Hsp90-Ligand 9	Ile33, Asn35, Ser36, Ser37, Ala39, Leu40, Ile43, Val76, Thr78, Ile80, Gly81, Met82, Thr83, Leu91, Gly92, Thr93, Ile94, Tyr123, Lys137, Thr168, Lys169, Ile171
Hsp90-Ligand 10	Ile33, Asn35, Ser36, Ser37, Ala39, Leu40, Ile43, Val76, Thr78, Ile80, Gly81, Met82, Thr83, Leu87, Gly92, Thr93, Ile94, Val120, Tyr123, Lys137, Lys169, Ile171
Hsp90-Ligand 22	Gln7, Ser36, Ser37, Ala39, Leu40, Ile43, Thr78, Ile80, Gly81, Met82, Thr83, Leu87, Ile88, Gly92, Thr93, Lys96, Val120, Gly121, Phe122, Tyr123, Ser124, Ile135, Lys137, Glu147, Thr168, Lys169, Ile171
Hsp90-Ligand 31	Ile34, Ser37, Ser38, Leu41, Val77, Thr79, Ile81, Gly82, Met83, Thr84, Ile89, Gly93, Ile95, Tyr124, Ile136, Lys138, Lys170, Ile172
Hsp90-Ligand 37	Gln7, Ile33, Asn35, Ser36, Ser37, Ala39, Leu40, Ile43, Val76, Thr78, Ile80, Gly81, Met82, Thr83, Leu87, Ile88, Gly92, Thr93, Ala95, Val120, Gly121, Phe122, Tyr123, Ser124, Thr133, Ile135, Lys137, Glu147, Thr168, Lys169, Ile171
Hsp90-Ligand 43	Ile33, Asn35, Ser36, Ser37, Ala39, Leu40, Ile43, Val76, Thr78, Ile80, Gly81, Met82, Thr83, Leu87, Ile88, Gly92, Thr93, Ala95, Val120, Gly121, Tyr123, Thr133, Ile135, Lys137, Glu147, Thr168, Lys169, Ile171
Hsp90-Ligand 58	Gln7, Ala11, Ile33, Ser36, Ser37, Ala39, Leu40, Thr78, Ile80, Gly81, Met82, Thr83, Leu87, Ile88, Gly92, Thr93, Lys96, Gly121, Tyr123, Ser124, Ile135, Lys137, Glu147, Thr168, Lys169, Ile171
Hsp90-Ligand 58	Gln7, Ile33, Ser36, Ser37, Leu40, Ile43, Thr78, Ile80, Gly81, Met82, Thr83, Leu87, Ile88, Gly92, Ala95, Tyr123, Ser124, Ile135, Lys137, Glu147, Lys169, Ile171
Hsp90-Ligand 62	Gln7, Ile33, Ser36, Ser37, Ala39, Leu40, Ile43, Thr78, Ile80, Gly81, Met82, Thr83, Lys84, Leu87, Ile88, Leu91, Gly92, Ala95, Val120, Tyr123, Ser124, Ile135, Asn139, Glu147, Lys169, Ile171
Hsp90-Ligand 65	Ile33, Ser36, Ser37, Ala39, Leu40, Ile43, Thr78, Ile80, Gly81, Met82, Thr83, Leu87, Ile88, Leu91, Gly92, Ala95, Lys96, Gly121, Tyr123, Ser124, Ile135, Lys137, Glu147, Thr168, Lys169, Ile171
Hsp90-Ligand 67	Gln7, Ile33, Ser36, Ser37, Leu40, Thr78, Ile80, Gly81, Met82, Thr83, Leu87, Ile88, Gly92, Lys96, Tyr123, Ser124, Ile135, Glu147, Lys169, Ile171
Hsp90-Ligand 70	Ile33, Asn35, Ser36, Ser37, Ala39, Leu40, Ile43, Val76, Thr78, Ile80, Gly81, Met82, Thr83, Leu87, Ile88, Gly92, Ala95, Val120, Gly121, Phe122, Tyr123, Ser124, Ile135, Lys137, Asn139, Lys169, Ile171

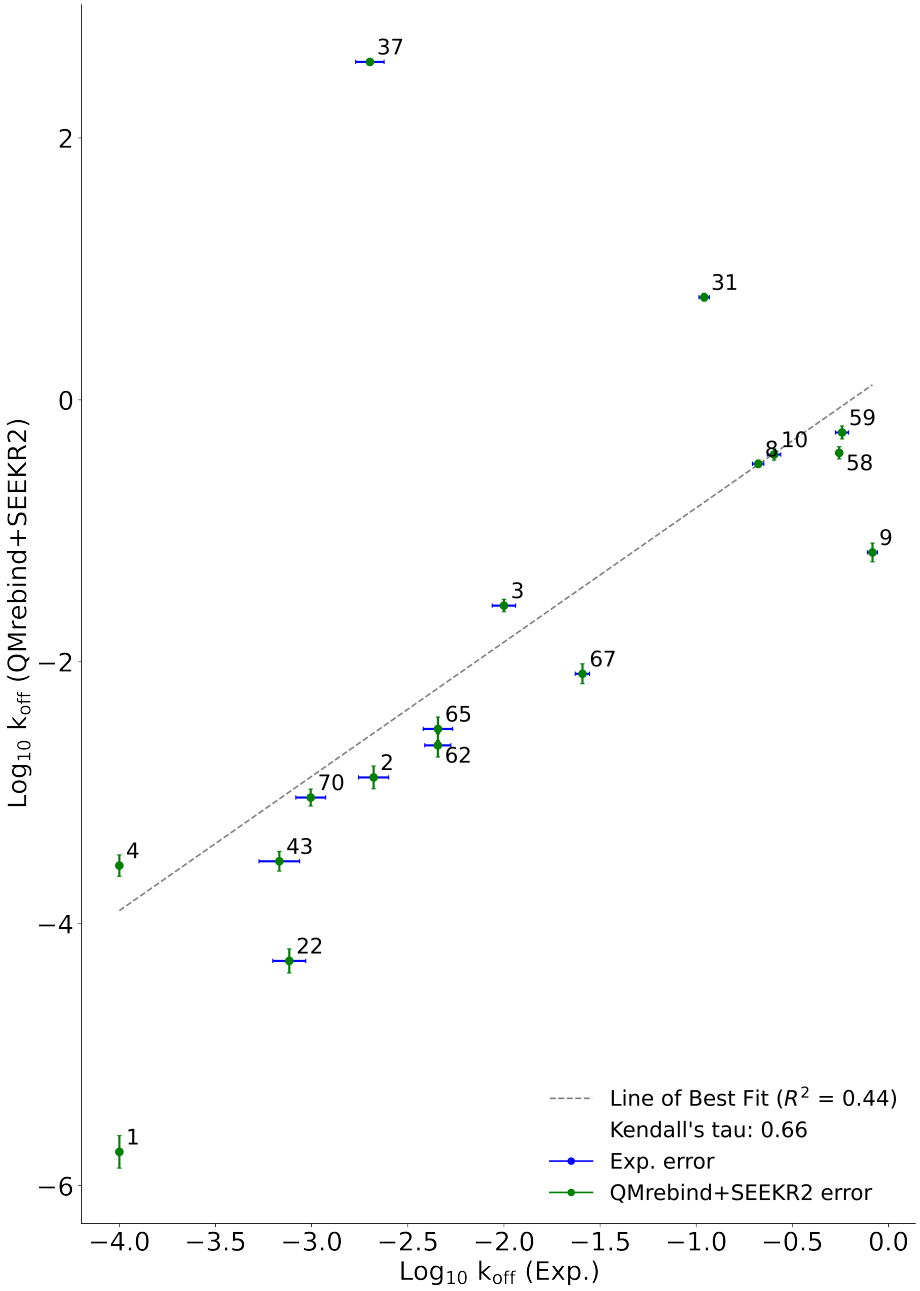

Figure S2: Scatter plot comparing the logarithm of experimental k_{off} values against the QMrebind+SEEKR2 estimated k_{off} values for Hsp90-inhibitor complexes. Each data point is labeled with its corresponding Hsp90-inhibitor complex ID, and error bars are shown for both data sets. The plot displays a line of best fit to indicate the correlation between the experimental and theoretically calculated k_{off}, with R^2 values indicating the goodness of the fit and the computed Kendall's tau statistic, denoting the strength and direction of the ordinal association between the experimental k_{off} and the QMrebind+SEEKR2 estimated k_{off} values for Hsp90-Inhibitor complexes. In this plot, the R^2 and Kendall's tau statistics included the outlier, compound 37, unlike Fig. 9 in the main text.

Table S3: Unbinding rate constants or k_{off} (s^{-1}) for eight Hsp90-inhibitor complexes obtained from experiments, QMrebind-reparameterized force field, and the generic force field parameters employed in SEEKR2 simulations.

Hsp90-inhibitor complex	Experimental k_{off} (s^{-1})	QMrebind+SEEKR2 k_{off} (s^{-1})	SEEKR2 k_{off} (s^{-1})
Hsp90-Ligand 1	$< 1.000 \times 10^{-4}$	$(1.8 \pm 0.6) \times 10^{-6}$	$(9. \pm 4.) \times 10^{-8}$
Hsp90-Ligand 4	$< 1.000 \times 10^{-4}$	$(2.8 \pm 0.8) \times 10^{-4}$	$(3.89 \pm 0.07) \times 10^{0}$
Hsp90-Ligand 22	$(7.6 \pm 0.5) \times 10^{-4}$	$(5. \pm 2.) \times 10^{-5}$	$(3. \pm 1.) \times 10^{-7}$
Hsp90-Ligand 3	$(1.00 \pm 0.09) \times 10^{-2}$	$(2.7 \pm 0.4) \times 10^{-2}$	$(4.9 \pm 0.8) \times 10^{2}$
Hsp90-Ligand 67	$(3. \pm 1.) \times 10^{-2}$	$(8.1 \pm 0.2) \times 10^{-3}$	$(1.413 \pm 0.009) \times 10^{-3}$
Hsp90-Ligand 31	$(1.1 \pm 0.4) \times 10^{-1}$	$(6.08 \pm 0.03) \times 10^{0}$	$(9.53 \pm 0.04) \times 10^{3}$
Hsp90-Ligand 59	$(5.73 \pm 0.02) \times 10^{-1}$	$(5.64 \pm 0.03) \times 10^{-1}$	$(4.18 \pm 0.04) \times 10^{-3}$
Hsp90-Ligand 9	$(8.2 \pm 0.5) \times 10^{-1}$	$(6.84 \pm 0.03) \times 10^{-2}$	$(5.01 \pm 0.02) \times 10^{-2}$

Table S4: Unbinding rate constants or k_{off} (s^{-1}) for 17 Hsp90-inhibitor complexes (with references) obtained from experiments and QMrebind-reparameterized force field parameters employed in SEEKR2 simulations.

Hsp90-inhibitor complex	Exp. k_{off} (s^{-1})	Exp. k_{off} reference	QMrebind+SEEKR2 k_{off} (s^{-1})
Hsp90-Ligand 1	$< 1.000 \times 10^{-4}$	[1]	$(1.8 \pm 0.6) \times 10^{-6}$
Hsp90-Ligand 4	$< 1.000 \times 10^{-4}$	[1]	$(2.8 \pm 0.8) \times 10^{-4}$
Hsp90-Ligand 43	$(6.80 \pm 0.05) \times 10^{-4}$	[2]	$(3. \pm 2.) \times 10^{-4}$
Hsp90-Ligand 22	$(7.6 \pm 0.5) \times 10^{-4}$	[1]	$(5. \pm 2.) \times 10^{-5}$
Hsp90-Ligand 70	$(10. \pm 1.) \times 10^{-4}$	[1]	$(9. \pm 6.) \times 10^{-4}$
Hsp90-Ligand 37	$(2.0 \pm 0.2) \times 10^{-3}$	[1]	$(3.82 \pm 0.05) \times 10^{2}$
Hsp90-Ligand 2	$(2.1 \pm 0.1) \times 10^{-3}$	[1]	$(1.31 \pm 0.05) \times 10^{-3}$
Hsp90-Ligand 62	$(4.5 \pm 0.4) \times 10^{-3}$	[1]	$(2.30 \pm 0.03) \times 10^{-3}$
Hsp90-Ligand 65	$(4.5 \pm 0.2) \times 10^{-3}$	[1]	$(3.08 \pm 0.03) \times 10^{-3}$
Hsp90-Ligand 3	$(1.00 \pm 0.09) \times 10^{-2}$	[1]	$(2.7 \pm 0.4) \times 10^{-2}$
Hsp90-Ligand 67	$(3. \pm 1.) \times 10^{-2}$	[1]	$(8.1 \pm 0.2) \times 10^{-3}$
Hsp90-Ligand 31	$(1.1 \pm 0.4) \times 10^{-1}$	[3]	$(6.08 \pm 0.03) \times 10^{0}$
Hsp90-Ligand 8	$(2.1 \pm 0.3) \times 10^{-1}$	[3]	$(3.2 \pm 0.4) \times 10^{-1}$
Hsp90-Ligand 10	$(2.5 \pm 0.2) \times 10^{-1}$	[1]	$(3.83 \pm 0.07) \times 10^{-1}$
Hsp90-Ligand 58	$(6. \pm 2.) \times 10^{-1}$	[2]	$(3.94 \pm 0.05) \times 10^{-1}$
Hsp90-Ligand 59	$(5.7 \pm 0.2) \times 10^{-1}$	[2]	$(5.64 \pm 0.03) \times 10^{-1}$
Hsp90-Ligand 9	$(8.2 \pm 0.5) \times 10^{-1}$	[1]	$(6.84 \pm 0.03) \times 10^{-2}$

Table S5: Residues of Hsp90 protein interacting with ligands 1 and 9 within a cut-off distance of 4 Å

Hsp90-inhibitor complex	Simulation time	Interacting residues
Hsp90-Ligand 1	10 µs	Leu33, Asn36, Ser37, Asp39, Ala40, Lys43, Asp78, Ile81, Gly82, Met83, Thr84, Asp87, Leu92, Gly93, Thr94, Ile95, Gly120, Phe123, Val135, Hie139, Thr169, Val171
Hsp90-Ligand 1	6 µs (0 - 6 µs)	Leu33, Asn36, Ser37, Asp39, Ala40, Lys43, Asp78, Ile81, Gly82, Met83, Leu92, Gly93, Thr94, Ile95, Gly120, Phe123, Val135, Hie139, Thr169, Val171
Hsp90-Ligand 1	2 µs (6.50 - 8.50 µs)	Leu33, Asn36, Ser37, Asp39, Ala40, Lys43, Asp78, Ile81, Gly82, Met83, Thr84, Asp87, Leu92, Gly93, Thr94, Gly120, Val121, Gly122, Phe123, Tyr124, Val135, Hie139, Thr169, Val171
Hsp90-Ligand 9	10 µs	Leu32, Asn35, Ser36, Asp38, Ala39, Lys42, Asp77, Ile80, Gly81, Met82, Leu91, Gly92, Thr93, Phe122, Thr136, Thr168, Val170

Table S6: Contact frequencies of Hsp90 residues when interacting with ligand 1 (within the ligand-binding pocket) over two intervals, i.e., 0 - 6 μs and 6.5 - 8.5 μs. These intervals are chosen based on the consistency and distinctness of the COM-COM distances between the ligand and the Hsp90 receptor within each interval. Here, contact frequencies are expressed as a percentage of the total number of possible contacts.

Hsp90 residues	Ligand 1 - residue contacts from 0 -6 μs (%)	Ligand 1 - residue contacts from 6.5 -8.5 μs (%)
Glu32	99.80	100.00
Ser35	100.00	100.00
Asn36	100.00	100.00
Ser38	99.07	97.00
Asp39	100.00	100.00
Asp42	99.00	98.20
Val77	100.00	100.00
Gly80	100.00	100.00
Ile81	100.00	100.00
Gly82	100.00	100.00
Met83	55.33	85.40
Ala86	82.47	94.20
Asn91	100.00	100.00
Leu92	99.67	98.20
Gly93	99.93	100.00
Thr94	98.00	38.80
Phe119	95.87	100.00
Gly120	7.80	100.00
Val121	4.20	99.00
Gly122	100.00	100.00
Phe123	0.00	97.20
Thr134	99.67	100.00
Ile136	24.27	5.80
Lys138	93.00	98.20
Gly168	100.00	100.00
Lys170	100.00	100.00
Lys209	100.00	100.00

References

(1) Kokh, D. B.; Amaral, M.; Bomke, J.; Gradler, U.; Musil, D.; Buchstaller, H.-P.; Dreyer, M. K.; Frech, M.; Lowinski, M.; Vallee, F., et al. Estimation of drug-target residence times by τ-random acceleration molecular dynamics simulations. *Journal of chemical theory and computation* **2018**, *14*, 3859–3869.

(2) Schuetz, D. A.; Richter, L.; Amaral, M.; Grandits, M.; Gradler, U.; Musil, D.; Buchstaller, H.-P.; Eggenweiler, H.-M.; Frech, M.; Ecker, G. F. Ligand desolvation steers on-rate and impacts drug residence time of heat shock protein 90 (Hsp90) inhibitors. *Journal of Medicinal Chemistry* **2018**, *61*, 4397–4411.

(3) Amaral, M.; Kokh, D.; Bomke, J.; Wegener, A.; Buchstaller, H.; Eggenweiler, H.; Matias, P.; Sirrenberg, C.; Wade, R.; Frech, M. Protein conformational flexibility modulates kinetics and thermodynamics of drug binding. *Nature communications* **2017**, *8*, 2276.